Solid-state emitter embedded in a microcavity under intense excitation: A variational master-equation approach

Oscar J. Gómez-Sánchez[1,2] and Hanz Y. Ramírez[1,*]

[1]*Grupo de Física Teórica y Computacional, Escuela de Física, Universidad Pedagógica y Tecnológica de Colombia, Tunja 150003, Boyacá, Colombia*
[2]*Department of Electrophysics, National Chiao Tung University, Hsinchu 30050, Taiwan*

In this work, dissipative effects from a phonon bath on the resonance fluorescence of a solid-state two-level system embedded in a high-quality semiconductor microcavity and driven by an intense laser are investigated. Within the density operator formalism, we derive a variational master equation valid for broader ranges of temperatures, pumping rates, and radiation-matter couplings than previous studies. From the obtained master equation, fluorescence spectra for various thermal and exciting conditions are numerically calculated and compared to those computed from weak coupling and polaronic master equations, respectively. Our results evidence the breakdown of those rougher approaches under increased temperature and strong pumping.

I. INTRODUCTION

Solid-state emitters embedded in microcavities have become a new paradigm in cavity quantum electrodynamics [1–3]. Recent developments in fabrication of semiconductor cavities serve a number of research fields, including quantum information processing, photonic circuits, and quantum optics [4–8]. Regarding the latter, high-quality cavities have been crucial for boosting the efficiency of single-photon generators [9–11].

For instance, some recent experimental studies have focused on the resonant fluorescence of InGaAs quantum dots (QDs) grown inside microcolumns, which have provided a clear demonstration of induced excitation [12–14]. Thus, in systems with nonresonant laser-cavity coupling, the cavity mode is indirectly excited by the emission of photons from an artificial atom coupled to the acoustic-phonon environment (phonon-assisted cavity feeding) [15,16]. The inverse effect of nonresonant coupling, where the quantum emitter is excited by photons emitted from the cavity, has also been observed [17].

McCutcheon *et al.* developed a variational master equation to describe the dynamics of a cavityless two-level system interacting with a boson environment, which was applied in the study of Rabi's rotations of a quantum dot [18]. They found that a variational-master-equation technique captures effects generally considered nonperturbative, such as multiphoton processes and renormalization of the Rabi frequency induced by the phonon bath. By comparing their population dynamics results with path-integral numerical calculations, the reliability of the variational approach in accounting for those nonperturbative effects, in regimes in which the weak and polaronic models are accurate, was verified.

Nevertheless, state-of-the-art experiments use optical resonators embedding the emitter, because of the associated improvement in collection rates and photon purity [10,19–23]. Thus, our purpose is to investigate the fluorescence spectrum of a solid-state qubit-cavity system under pumping and thermal conditions beyond the scope of previously studied formulations such as the weak-coupling and polaronic approaches. To do that, we derive a variational master equation, which allows for numerical simulations of resonance fluorescence spectra within a wider range of excitation rates, emitter-cavity couplings, and temperatures. Such a master equation might also contribute to the promising research on double-dot–cavity systems, regarding phonon dissipation in tunnel-coupled emitters [24–28].

Although this kind of system has been addressed by means of numerical approaches, which, adequately implemented, may render a solution as close as desired to the exact one (e.g., quasiadiabatic propagator path-integral or real-time path-integral techniques) [18,29–32], those techniques are highly demanding from a computational point of view and do not yield the physical insight provided by a master equation.

This paper is organized as follows. In the next section we present the model Hamiltonian and its modification under an adequate unitary transformation. In Sec. III the free energy of the system is minimized to determine the variational parameters and in Sec. IV the corresponding variational master equation is derived. In Sec. V we obtain and discuss numerical simulations of fluorescence spectra of a semiconductor QD coupled to a cavity mode. We summarize and draw conclusions in Sec. VI.

II. THEORY

The system under study is a solid-state two-level system (which we will refer to as a quantum dot, although it could be a vacancy in a three-dimensional crystal, a localized defect in a low-dimensional structure, a nanocrystal, or any other
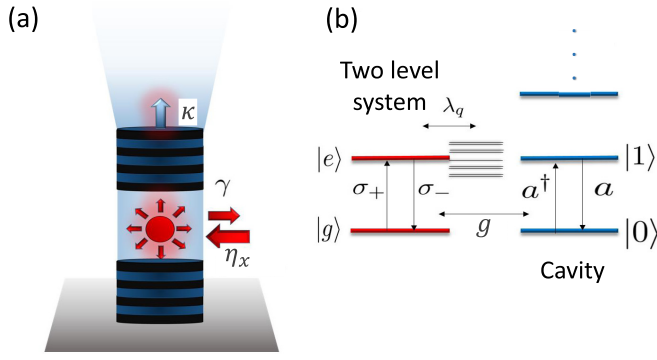
———————
*hanz.ramirez@uptc.edu.co

FIG. 1. (a) Schematics of a quantum emitter (pure radiative linewidth γ), embedded in a micropillar cavity (loss rate κ) and driven by a laterally applied cw laser (pumping rate η_x). (b) Emitter energy levels (ground $|g\rangle$ and excited $|e\rangle$) and their interactions with the phonon reservoir (phonon-exciton coupling λ_q) and the cavity (light-matter coupling g).

suitable artificial atom), embedded in a QED cavity [33]. Carriers confined in the QD interact with a continuum of states in the sample of which it is part, via acoustic phonons. This interaction causes an incoherent pumping of the two-level system. Moreover, because the artificial atom mainly interacts with a single mode of the cavity, the phonon environment produces some decoherence effects in the atom-cavity arrangement. The system is assumed to be driven by a cw laser, as shown in Fig. 1(a), with the corresponding energy levels and interactions depicted in Fig. 1(b).

Working in a rotating frame whose frequency matches that of the exciting laser ω_L [34,35], the considered Hamiltonian reads ($\hbar = 1$)

$$
\begin{aligned}
\hat{H} = {} & \Delta_{XL}\hat{\sigma}^+\hat{\sigma}^- + \Delta_{CL}\hat{a}^\dagger\hat{a} \\
& + \eta_x(\hat{\sigma}^+ + \hat{\sigma}^-) + g(\hat{\sigma}^+\hat{a} + \hat{a}^\dagger\hat{\sigma}^-) \\
& + \hat{\sigma}^+\hat{\sigma}^- \sum_q \lambda_q(\hat{b}_q + \hat{b}_q^\dagger) + \sum_q \omega_q \hat{b}_q^\dagger \hat{b}_q,
\end{aligned} \tag{1}
$$

where ω_q is the frequency of a phonon with momentum q, and b_q ($\hat{b}_q^\dagger$) and λ_q are the boson annihilation (creation) operator and intensity of the carrier-phonon coupling, respectively. The detuning with respect to the pumping laser of the two-level transition frequency ω_X and that of the cavity mode ω_C are, respectively, Δ_{CL} and Δ_{XL}. The annihilation (creation) operator of photons at the cavity frequency is $\hat{a}$ ($\hat{a}^\dagger$) and the QD dipole operators are σ^- and σ^+. In addition, g is the radiation-matter coupling constant and the pumping rate η_x is the half of the Rabi frequency associated with the driving laser power.

Let us consider a generalization of the polaron transformation that displaces the phonon bath oscillators, by an amount that is determined by a set of variational parameters $\{f_q\}$ [18]. Such a variational transformation can be written as

$$
\hat{H}' = e^{\hat{S}}\hat{H}e^{-\hat{S}}, \tag{2}
$$

where

$$
\hat{S} = \hat{\sigma}^+\hat{\sigma}^- \sum_q \nu_q(\hat{b}_q^\dagger - \hat{b}_q), \tag{3}
$$

where $\nu_q = \frac{f_q}{\omega_q}$. The transformed Hamiltonian becomes $\hat{H}'_S + \hat{H}'_I + \hat{H}'_B$, with

$$
\hat{H}'_S = \Delta_R\hat{\sigma}^+\hat{\sigma}^- + \Delta_{CL}\hat{a}^\dagger\hat{a} + \langle\hat{B}\rangle\hat{\xi}_x, \tag{4}
$$

$$
\hat{H}'_I = \sum_{i=x,y,z} \hat{\xi}_i \hat{B}_i, \tag{5}
$$

$$
\hat{H}'_B = \sum_q \omega_q \hat{b}_q^\dagger \hat{b}_q, \tag{6}
$$

where the modified detuning $\Delta_R = \Delta_{XL} + R$ depends on the variational shift $R = \sum_q \omega_q^{-1} f_q(f_q - 2\lambda_q)$ and the thermal average of the bath displacement operator is given by (with $\beta = 1/k_B T$)

$$
\langle\hat{B}\rangle = \exp\left[-\frac{1}{2}\sum_q \frac{f_q^2}{\omega_q^2}\coth(\beta\omega_q/2)\right]. \tag{7}
$$

In turn, the system modified operators $\hat{\xi}_i$ are explicitly

$$
\hat{\xi}_x = \eta_x(\hat{\sigma}^+ + \hat{\sigma}^-) + g(\hat{\sigma}^+\hat{a} + \hat{\sigma}^-\hat{a}^\dagger), \tag{8}
$$

$$
\hat{\xi}_y = i\eta_x(\hat{\sigma}^+ - \hat{\sigma}^-) + ig(\hat{\sigma}^+\hat{a} - \hat{\sigma}^-\hat{a}^\dagger), \tag{9}
$$

$$
\hat{\xi}_z = \hat{\sigma}^+\hat{\sigma}^- \tag{10}
$$

and the phonon-induced fluctuation operators are defined as

$$
\hat{B}_x = \tfrac{1}{2}(\hat{B}_+ + \hat{B}_- - 2\langle\hat{B}\rangle), \tag{11}
$$

$$
\hat{B}_y = \frac{1}{2i}(\hat{B}_+ - \hat{B}_-), \tag{12}
$$

$$
\hat{B}_z = \sum_q (\lambda_q - f_q)(\hat{b}_q^\dagger + \hat{b}_q) \tag{13}
$$

in terms of the coherent displacement operators

$$
\hat{B}_\pm = \exp\left(\pm\sum_q \nu_q(\hat{b}_q^\dagger - \hat{b}_q)\right). \tag{14}
$$

In the limit of continuous phonon modes, which is convenient and appropriate as long as the lattice parameter is much smaller than the typical size of the sample embedding the emitter, a spectral density $J(\omega)$ must be introduced so that $\langle B\rangle$ and R correspondingly turn into

$$
R = \int_0^\infty d\omega \frac{J(\omega)}{\omega} F(\omega)[F(\omega) - 2], \tag{15}
$$

$$
\langle B\rangle = \exp\left[-\frac{1}{2}\int_0^\infty d\omega \frac{J(\omega)^2 F(\omega)^2}{\omega^2}\coth(\beta\omega/2)\right]. \tag{16}
$$

III. FREE-ENERGY MINIMIZATION

The variational parameters $\{f_q\}$ must be chosen in such a way that they minimize the free energy associated with the transformed Hamiltonian [36–38]. To do that, we use the Feynman-Bogoliubov inequality $A_u \geqslant A$, according which

the free energy of the system (A) is at first order bounded by an upper limit given by

$$A_u = -\frac{1}{\beta} \ln(\text{Tr}\{e^{-\beta \hat{H}_0'}\}) + \langle \hat{H}_I' \rangle_{\hat{H}_0'}, \qquad (17)$$

where $\hat{H}_0' = \hat{H}_S' + \hat{H}_B'$ and $\langle \hat{H}_I' \rangle_{\hat{H}_0'} = \text{Tr}\{\hat{H}_I' e^{-\beta \hat{H}_0'}\}$.

On the one hand, $\langle \hat{H}_I' \rangle_{\hat{H}_0'}$ vanishes because in the basis of eigenstates of $\hat{H}_0'$, all diagonal terms of $\hat{H}_I'$ are zero. On the

other hand, since $[\hat{H}_B', \hat{H}_S'] = 0$ and each of those operators acts on eigenstates of different subspaces (the dot-cavity and the phonon bath), then A_u can be reduced to

$$A_u = A_B - \frac{1}{\beta} \ln(\text{Tr}\{e^{-\beta \hat{H}_S'}\}), \qquad (18)$$

with A_B the free energy of the phonon bath. Inserting Eq. (4) into Eq. (17), the Feynman-Bogoliubov upper bound reads

$$A_u = A_B - \frac{1}{\beta} \ln \left\{ 2 e^{-(\beta/2)[(2n-1)\Delta_{CL} + \Delta_R]} \left[\cosh \left(\frac{1}{2} \beta \mu_1 \right) + \cosh \left(\frac{1}{2} \beta \mu_2 \right) \right] \right\} \qquad (19)$$

in terms of the phonon mean occupation number at temperature T ($n = \langle \hat{b}^\dagger \hat{b} \rangle = [e^{\beta\omega} - 1]^{-1}$) and of the quantities

$$\mu_1 = \sqrt{\mho_1 + 2\mho_2}, \quad \mu_2 = \sqrt{\mho_1 - 2\mho_2}, \qquad (20)$$

which in turn depend on

$$\mho_1 = \Delta_{CL}^2 + \Delta_R^2 + 2B^2(g^2 n + 2\eta_x^2),$$

$$\mho_2 = \sqrt{(B^2 g^2 n - \Delta_{CL}\Delta_R)^2 + 4B^2(B^2 g^2 n + \Delta_{CL}^2)\eta_x^2}.$$

Because the free energy of the phonon bath does not depend on f_q, i.e., A_B is unchanged by the interaction with the system, it is irrelevant in minimizing A_u. By imposing $\frac{\partial A_u}{\partial f_q} = 0$, we obtain

$$f_q \equiv \lambda_q F(\omega_q) = \frac{\lambda_q \left(1 - \frac{\frac{\Delta_R + \Lambda_2}{\mu_1} \sinh(\beta\mu_1/2) + \frac{\Delta_R - \Lambda_2}{\mu_2} \sinh(\beta\mu_2/2)}{\cosh(\beta\mu_1/2) + \cosh(\beta\mu_2/2)}\right)}{1 - \frac{\frac{\Delta_R + \Lambda_2}{\mu_1} \sinh(\beta\mu_1/2) + \frac{\Delta_R - \Lambda_2}{\mu_2} \sinh(\beta\mu_2/2)}{\cosh(\beta\mu_2/2) + \cosh(\beta\mu_2/2)} + \frac{B^2}{\omega_q} \frac{\frac{(ng^2 + 2\eta_x^2) + \Lambda_1}{\mu_1} \sinh(\beta\mu_1/2) + \frac{(ng^2 + 2\eta_x^2) - \Lambda_1}{\mu_2} \sinh(\beta\mu_2/2)}{\cosh(\beta\mu_2/2) + \cosh(\beta\mu_2/2)} \coth(\beta\omega_q/2)}, \qquad (21)$$

where $\Lambda_1 = \frac{B^2 g^2 n(g^2 n + 4\eta_x^2) - \Delta_{CL}(g^2 n \delta_R - 2\Delta_{CL}\eta_x^2)}{\mho_2}$ and $\Lambda_2 = \frac{\Delta_{CL}(\Delta_{CL}\Delta_R - B^2 g^2 n)}{\mho_2}$.

In Fig. 2 the frequency dependence of the modulating part of the variational parameters for different pumping rates, radiation-matter couplings, and temperatures is presented. It can be seen how for wave vectors q, whose associated frequencies satisfy $\eta_x/\omega_q \ll 1$, the minimization condition yields $f_q \to \lambda_q$, recovering the polaronic limit [38]. Only for these modes can the bath oscillators fully follow the atom excitation. Otherwise, the mode frequencies are too slow and the corresponding oscillator shifts dwindle, so the carrier-phonon coupling at the corresponding momentum range is inhibited.

IV. MASTER EQUATION

In this section, a variational master equation for the reduced density operator $\hat{\rho}(t)$, of the QD-cavity system, is derived within the second-order Born-Markov framework [39]. The use of those approximations is justified because even at room temperature, the thermal energy would be much smaller than the typical transition energy of the two-level emitter and the thermalization processes are much faster than the relevant optical dynamics [40]. The validity of convolutionless non-perturbative approaches (regarding the phonon-carrier inter-action) for studying strongly coupled dot-cavity systems has been shown in Refs. [35,41]. In the case of strong pumping, minimization of the free energy is expected to catch relevant non-Markovian effects.

We include the emitter radiative recombination and the cavity losses as Liouvillian decay superoperators, which act on the density matrix of the reduced system [42]. Such operators in the Lindblad form are given by

$$\mathcal{L}(\hat{\rho}) = \frac{\gamma}{2}(2\hat{\sigma}^- \hat{\rho} \hat{\sigma}^+ - \hat{\sigma}^+ \hat{\sigma}^- \hat{\rho} - \hat{\rho}\hat{\sigma}^+ \hat{\sigma}^-)$$
$$+ \kappa(2\hat{a}\hat{\rho}\hat{a}^\dagger - \hat{a}^\dagger \hat{a}\hat{\rho} - \hat{\rho}\hat{a}^\dagger \hat{a}), \qquad (22)$$

where $\gamma/2$ is the HWHM radiative linewidth and κ is the cavity loss rate for the relevant mode. Thus, inserting the transformed Hamiltonian from Eqs. (4)–(6), the variational master equation takes the form

$$\frac{\partial \hat{\rho}}{\partial t} = -i[H_s, \hat{\rho}(t)] + \mathcal{L}(\hat{\rho})$$
$$- \int_0^t d\tau \sum_{\substack{l=x,y,z \\ m=x,y,z}} C_{lm}[\hat{\xi}_m, e^{-iH_s\tau}\hat{\zeta}_l e^{iH_s\tau}\hat{\rho}(t)]$$
$$+ \int_0^t d\tau \sum_{\substack{l=x,y,z \\ m=x,y,z}} C_{lm}^*[\hat{\rho}(t)e^{-iH_s\tau}\hat{\zeta}_l e^{iH_s\tau}, \hat{\xi}_m], \qquad (23)$$

where $C_{lm}(\tau) = \langle B_l(\tau)B_m \rangle$ for $l, m = x, y, z$. Assuming that the phonon bath is in thermal equilibrium [43], the correlation functions become

$$C_{xx}(\tau) = \langle B \rangle^2 \sin \phi(\tau),$$
$$C_{yy}(\tau) = \langle B \rangle^2 [\cos \phi(\tau) - 1],$$

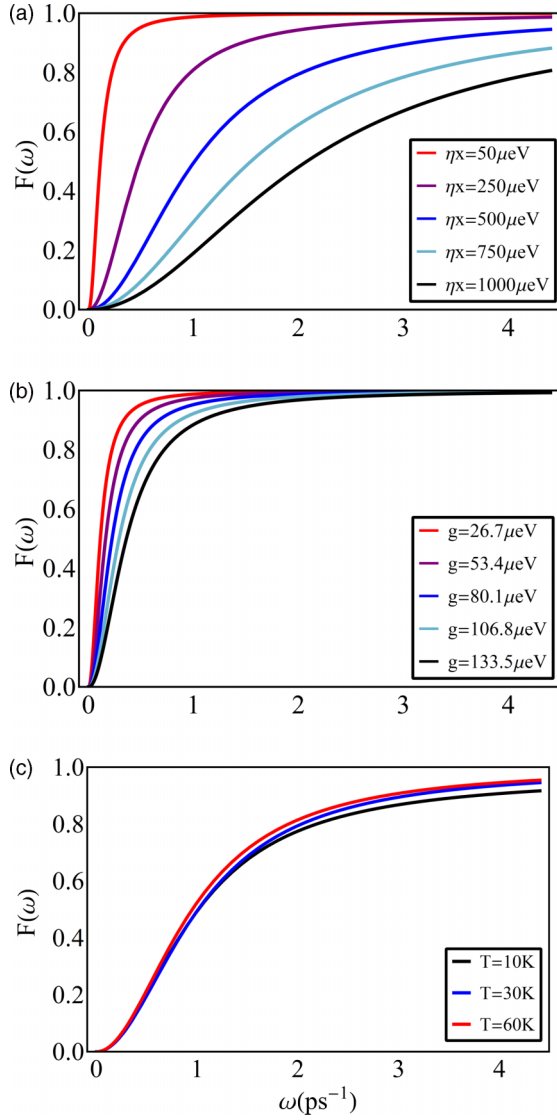FIG. 2. Variational parameter as a function of the phonon frequency at (a) $T = 30$ K and $g = 26.7$ μeV for different pumping rates (from bottom to top, the curves correspond to smaller rates), (b) $T = 30$ K and $\eta_x = 100$ μeV for different coupling constants (from bottom to top, the curves correspond to smaller couplings), and (c) $\eta_x = 500$ μeV and $g = 26.7$ μeV for different temperatures (from bottom to top, the curves correspond to higher temperatures).

$$C_{zz}(\tau) = \int_0^\infty d\omega \, J(\omega)[1 - F(\omega)]^2$$
$$\times [\cos \omega\tau \coth(\beta\omega/2) - i \sin \omega\tau],$$
$$C_{zy}(\tau) = \langle B \rangle \int_0^\infty d\omega \frac{J(\omega)}{\omega} F(\omega)[1 - F(\omega)]$$
$$\times [i \cos \omega\tau + \sin \omega\tau \coth(\beta\omega/2)],$$
$$C_{yz}(\tau) = -\langle B_z(\tau) B_y(0) \rangle,$$
$$C_{xz}(\tau) = C_{zx}(\tau) = C_{xy}(\tau) = C_{yx}(\tau) = 0, \tag{24}$$

which depend on the spectral density and on the variational parameters. The first two correlations also depend on the

function

$$\phi(\tau) = \int_0^\infty d\omega \frac{J(\omega)}{\omega^2} F(\omega)^2 [\cos \omega\tau \coth(\beta\omega/2) - i \sin \omega\tau]. \tag{25}$$

On the other hand, the master equation can be written in the Lindblad form

$$\frac{\partial \hat{\rho}(t)}{\partial t} = -i \{ [H_S^{\text{eff}}, \hat{\rho}(t)] + D_{ph}(\hat{\rho}) \} + \mathcal{L}(\hat{\rho}) + \mathcal{L}_{ph}(\hat{\rho}), \tag{26}$$

in terms of the effective Hamiltonian that describes the coherent part of the system evolution

$$H_S^{\text{eff}} = \Delta_{xL}\hat{\sigma}^+\hat{\sigma}^- + \Delta_{cL}\hat{a}^\dagger a + \langle B \rangle \zeta_x + \Delta_W^{\hat{\sigma}_1 1}\hat{\sigma}^+\hat{\sigma}^-$$
$$+ \Delta_{ph}^{\hat{\sigma}^+\hat{a}}\hat{a}^\dagger\hat{\sigma}^-\hat{\sigma}^+\hat{a} + \Delta_{ph}^{\hat{\sigma}^-}\hat{\sigma}^-\hat{\sigma}^+$$
$$+ \Delta_{ph}^{\hat{a}^\dagger\hat{\sigma}^-} a\hat{\sigma}^+\hat{\sigma}^-\hat{a}^\dagger + \Delta_{ph}^{\hat{\sigma}^+}\hat{\sigma}^+\hat{\sigma}^- \tag{27}$$

and of the dissipative Lindbladian $\mathcal{L}_{ph}(\hat{\rho})$ and the coherent variational shift $D_{ph}(\hat{\rho})$. The former is defined according to

$$\mathcal{L}_{ph}(\hat{\rho}) = \frac{\Gamma_W^{\hat{\sigma}_{11}}}{2} L(\hat{\sigma}_{11}) + \mathcal{L}_{ph}^{\text{intp}} + \frac{\Gamma_{ph}^{\hat{\sigma}^+\hat{a}}}{2} L(\hat{\sigma}^+\hat{a}) + \frac{\Gamma_{ph}^{\hat{\sigma}^-}}{2} L(\hat{\sigma}^-)$$
$$+ \frac{\Gamma_{ph}^{\hat{a}^\dagger\hat{\sigma}^-}}{2} L(\hat{a}^\dagger\hat{\sigma}^-) + \frac{\Gamma_{ph}^{\hat{\sigma}^+}}{2} L(\hat{\sigma}^+), \tag{28}$$

where $\hat{\sigma}_{11} \equiv \hat{\sigma}^+\hat{\sigma}^-$ and $L(\hat{D}) = 2\hat{D}\hat{\rho}\hat{D}^\dagger - \hat{D}^\dagger\hat{D}\hat{\rho} - \hat{\rho}\hat{D}^\dagger\hat{D}$. The term $\mathcal{L}_{ph}^{\text{intp}}(\hat{\rho})$ describes the incoherent interpolation processes between the weak-coupling approach [44] and the polaronic theory [41] and explicitly reads

$$\mathcal{L}_{ph}^{\text{intp}}(\hat{\rho}) = \frac{\Gamma_{zy}^{\hat{\sigma}_{11}\hat{\sigma}^+}}{2} L_{ph}^{\text{intp}}(\hat{\sigma}_{11}, \hat{\sigma}^+) + \Gamma_{zy}^{\hat{\sigma}_{11}\hat{\sigma}^-} L_{ph}^{\text{intp}}(\hat{\sigma}_{11}, \hat{\sigma}^-)$$
$$+ \frac{\Gamma_{zy}^{\hat{\sigma}_{11}(\hat{\sigma}^+\hat{a})}}{2} L_{ph}^{\text{intp}}(\hat{\sigma}_{11}, \hat{\sigma}^+\hat{a})$$
$$+ \frac{\Gamma_{zy}^{\hat{\sigma}_{11}(\hat{\sigma}^-\hat{a}^\dagger)}}{2} L_{ph}^{\text{intp}}(\hat{\sigma}_{11}, \hat{\sigma}^-\hat{a}^\dagger)$$
$$+ \frac{\Gamma_{yz}^{\hat{\sigma}^+\hat{\sigma}_{11}}}{2} L_{ph}^{\text{intp}}(\hat{\sigma}^+, \hat{\sigma}_{11}) + \frac{\Gamma_{yz}^{\hat{\sigma}^-\hat{\sigma}_{11}}}{2} L_{ph}^{\text{intp}}(\hat{\sigma}^-, \hat{\sigma}_{11})$$
$$+ \frac{\Gamma_{yz}^{(\hat{\sigma}^+\hat{a})\hat{\sigma}_{11}}}{2} L_{ph}^{\text{intp}}(\hat{\sigma}^+\hat{a}, \hat{\sigma}_{11})$$
$$+ \frac{\Gamma_{yz}^{(\hat{\sigma}^-\hat{a}^\dagger)\hat{\sigma}_{11}}}{2} L_{ph}^{\text{intp}}(\hat{\sigma}^-\hat{a}^\dagger, \hat{\sigma}_{11}), \tag{29}$$

with $L_{ph}^{\text{intp}}(A, B) = AB\hat{\rho}(t) - \hat{\rho}(t)B^\dagger A^\dagger - B\hat{\rho}(t)A + A^\dagger\hat{\rho}(t)B^\dagger$. The variational coherent shift (which also originates from interpolation between the weak-coupling and polaronic models) [40] is given by

$$D_{ph}(\hat{\rho}) = \Delta_{zy}^{\hat{\sigma}_{11}\hat{\sigma}^+} \mathfrak{D}_{ph}^{\text{intp}}(\hat{\sigma}_{11}, \hat{\sigma}^+) + \Delta_{zy}^{\hat{\sigma}_{11}\hat{\sigma}^-} \mathfrak{D}_{ph}^{\text{intp}}(\hat{\sigma}_{11}, \hat{\sigma}^-)$$
$$+ \Delta_{zy}^{\hat{\sigma}_{11}\hat{\sigma}^+\hat{a}} \mathfrak{D}_{ph}^{\text{intp}}(\hat{\sigma}_{11}, \hat{\sigma}^+\hat{a})$$
$$+ \Delta_{zy}^{\hat{\sigma}_{11}\hat{\sigma}^-\hat{a}^\dagger} \mathfrak{D}_{ph}^{\text{intp}}(\hat{\sigma}_{11}, \hat{\sigma}^-\hat{a}^\dagger)$$
$$+ \Delta_{yz}^{\hat{\sigma}^+\hat{\sigma}_{11}} \mathfrak{D}_{ph}^{\text{intp}}(\hat{\sigma}^+, \hat{\sigma}_{11}) + \Delta_{yz}^{\hat{\sigma}^-\hat{\sigma}_{11}} \mathfrak{D}_{ph}^{\text{intp}}(\hat{\sigma}^-, \hat{\sigma}_{11})$$

$$+ \Delta_{yz}^{\hat{\sigma}^+\hat{a}\hat{\sigma}_{11}} \mathfrak{D}_{ph}^{\text{intp}}(\hat{\sigma}^+\hat{a}, \hat{\sigma}_{11})$$

$$+ \Delta_{yz}^{\hat{\sigma}^-\hat{a}^\dagger\hat{\sigma}_{11}} \mathfrak{D}_{ph}^{\text{intp}}(\hat{\sigma}^-\hat{a}^\dagger, \hat{\sigma}_{11}), \qquad (30)$$

where $\mathfrak{D}_{ph}^{\text{intp}}(A, B) = AB\hat{\rho}(t) + \hat{\rho}(t)B^\dagger A^\dagger - B\hat{\rho}(t)A - A^\dagger\hat{\rho}(t)B^\dagger$.

By comparing Eq. (23) with (26) and dropping highly oscillatory terms, we obtain the phonon-mediated transition probabilities and the variational shifts. The thermal dissipative rates are found to be of three types: weak-coupling-like rates [44,45]

$$\Gamma_W^{\hat{\sigma}_{11}} = 2\,\text{Re}\left[\int_0^\infty d\tau\, Czz(\tau)\right], \qquad (31)$$

polaronic-like rates [40]

$$\Gamma_{ph}^{\hat{\sigma}^+\hat{a}/\hat{a}^\dagger\hat{\sigma}^-} = 2g^2\text{Re}\left[\int_0^\infty d\tau\, \langle B\rangle^2 e^{\pm\Delta_{cx}\tau}(e^{\phi(\tau)} - 1)\right], \quad (32)$$

$$\Gamma_{ph}^{\hat{\sigma}^+/\hat{\sigma}^-} = 2\eta_x^2\text{Re}\left[\int_0^\infty d\tau\, \langle B\rangle^2 e^{\mp\Delta_{xL}\tau}(e^{\phi(\tau)} - 1)\right], \quad (33)$$

and interpolated rates

$$\Gamma_{zy}^{\hat{\sigma}_{11}\hat{\sigma}^\pm} = \mp 2\eta_x\,\text{Im}\left[\int_0^\infty d\tau\, C_{zy}(\tau)e^{\mp\Delta_{XL}\tau}\right], \qquad (34)$$

$$\Gamma_{zy}^{\hat{\sigma}_{11}(\hat{\sigma}^+\hat{a}/\hat{\sigma}^-\hat{a}^\dagger)} = \mp 2g\,\text{Im}\left[\int_0^\infty d\tau\, C_{zy}(\tau)e^{\pm\Delta_{cx}\tau}\right], \qquad (35)$$

$$\Gamma_{yz}^{\hat{\sigma}^\pm\hat{\sigma}_{11}} = \mp 2\eta_x\,\text{Im}\left[\int_0^\infty d\tau\, C_{yz}(\tau)\right], \qquad (36)$$

$$\Gamma_{yz}^{(\hat{\sigma}^+\hat{a}/\hat{\sigma}^-\hat{a}^\dagger)\hat{\sigma}_{11}} = \mp 2g\,\text{Im}\left[\int_0^\infty d\tau\, C_{yz}(\tau)\right]. \qquad (37)$$

Meanwhile, the energy shift components are identified as

$$\Delta_W^{\hat{\sigma}_{11}} = \text{Im}\left[\int_0^\infty d\tau\, Czz(\tau)\right], \qquad (38)$$

$$\Delta_{ph}^{\hat{\sigma}^+\hat{a}/\hat{a}^\dagger\hat{\sigma}^-} = g^2\text{Im}\left[\int_0^\infty d\tau\, \langle B\rangle^2 e^{\pm\Delta_{cx}\tau}(e^{\phi(\tau)} - 1)\right], \quad (39)$$

$$\Delta_{ph}^{\hat{\sigma}^+/\hat{\sigma}^-} = \eta_x^2\text{Im}\left[\int_0^\infty d\tau\, \langle B\rangle^2 e^{\mp\Delta_{xL}\tau}(e^{\phi(\tau)} - 1)\right], \quad (40)$$

$$\Delta_{zy}^{\hat{\sigma}_{11}\hat{\sigma}^\pm} = \pm\eta_x\text{Re}\left[\int_0^\infty d\tau\, C_{zy}(\tau)e^{\mp\Delta_{XL}\tau}\right], \qquad (41)$$

$$\Delta_{zy}^{\hat{\sigma}_{11}\hat{\sigma}^+\hat{a}/\hat{\sigma}^-\hat{a}^\dagger} = \pm g\,\text{Re}\left[\int_0^\infty d\tau\, C_{zy}(\tau)e^{\pm\Delta_{cx}\tau}\right], \qquad (42)$$

$$\Delta_{yz}^{\hat{\sigma}^\pm\hat{\sigma}_{11}} = \pm\eta_x\text{Re}\left[\int_0^\infty d\tau\, C_{yz}(\tau)\right], \qquad (43)$$

$$\Delta_{yz}^{\hat{\sigma}^+\hat{a}/\hat{\sigma}^-\hat{a}^\dagger\hat{\sigma}_{11}} = \pm g\,\text{Re}\left[\int_0^\infty d\tau\, C_{yz}(\tau)\right]. \qquad (44)$$

V. NUMERICAL RESULTS

As a representative study case, we will focus on the resonance fluorescence of an InAs/GaAs quantum dot coupled to a high-quality optical resonator, under resonant continuous-wave excitation [46,47]. It is known that in most III-V semiconductor materials, the main source of dephasing is the carrier–acoustic-phonon interaction via the deformation potential [48,49]. Thus, the spectral density $J_{ph}(\omega) = \alpha\omega^3 e^{-\omega^2/2\omega_b^2}$ is adopted for the simulations. Here α captures the strength of the exciton-phonon coupling and ω_b provides a natural high-frequency cutoff, which is proportional to the inverse of the carrier localization length in the QD [38].

To simulate the fluorescence spectrum, we compute

$$S_c(\omega) \propto \lim_{t\to\infty} \text{Re}\left[\int_0^\infty d\tau[\langle a(t+\tau)\hat{a}^\dagger(t)\rangle\right.$$
$$\left. - \langle a(t+\tau)\rangle\langle\hat{a}^\dagger(t)\rangle]e^{i(\omega_L - \omega)\tau}\right], \qquad (45)$$

where the correlation functions are obtained by the quantum regression formula [50]. To numerically solve the master equation within the different levels of approximation compared here (weak coupling, polaronic, and variational), we employ a quantum optics toolbox developed in MATLAB by Tan [51]. The pumping rate is assumed stable, i.e., η_x is taken to be independent of time, and the emitter is considered in the base state as the initial condition [52].

To make our results comparable to Mollow triplet experiments on semiconductor micropillars by Ulrich *et al.* [13], we consider a mode-cavity detuning $\omega_c - \omega_x = -0.2$ meV and a radiative decay rate $\gamma = 3$ μeV. These values are similar to the ones used in experiments by Hargart *et al.* in Ref. [14] and by Kim *et al.* in Ref. [53]. As for phonon parameters, typical values for InAs/GaAs QDs are used (cutoff frequency $\omega_b = 0.9$ meV and $\alpha_p = 0.03$ ps^2) [14,54,55].

Figure 3 shows emission spectra from the cavity for various pumping rates and temperatures, obtained within the three master-equation approaches considered. One can see how the weak-coupling model differs greatly from the polar and variational theories as the system temperature increases, because of overestimation of the phonon dissipative effects. Concurrently, as long as the pumping rate remains moderate (e.g., $\eta_x = 50$ μeV), the polar and variational approaches predict similar behaviors. In this regime, the polaron model has been successfully fitted to resonance fluorescence measurements [56]. However, contrasts between those two latter master equations are revealed when the pumping rate is strengthened. At median laser power (e.g., $\eta_x = 250$ μeV), the variational theory exhibits intermediate results between the weak-coupling and polaronic models, which is particularly observable at the Mollow triplet side peaks. Under high-excitation conditions (e.g., $\eta_x = 500$ μeV), the polaronic and variational approaches differ significantly in the predicted renormalization of the Rabi frequency and the emission intensity of all the peaks, especially the right one in the triplet, evidencing how in this regime the polaronic approach also overestimates the phonon-associated decoherence.

Such a breakdown of the polaronic approach for high pumping rates becomes larger as the temperature increases. Surprisingly, for strong pumping, as compared with the variational results, predictions from the weak-coupling model differ less than those from the polaronic model.

In order to check the consistency of our results with real-time path-integral calculations, we compare the Rabi
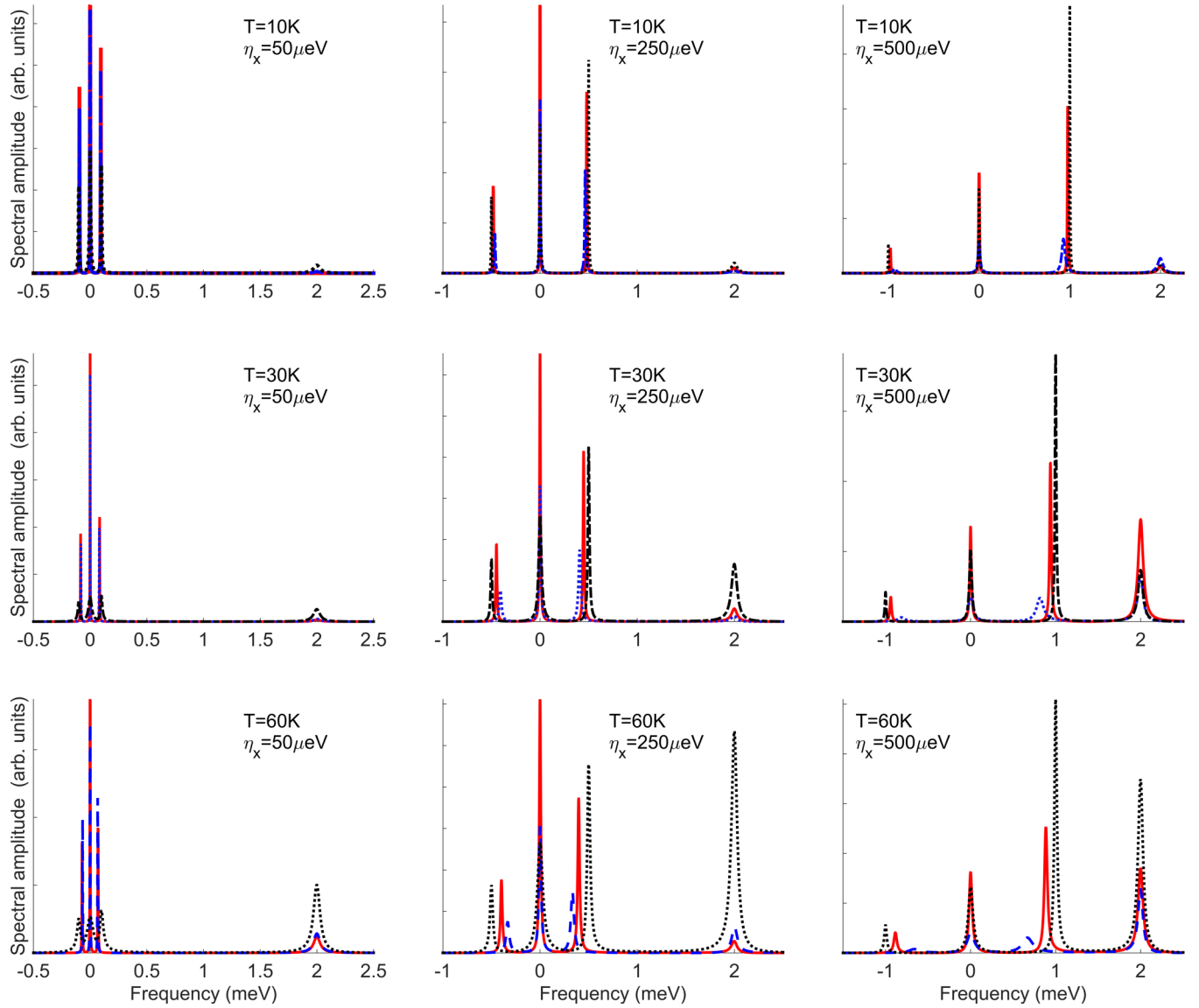
FIG. 3. Cavity-emitted fluorescence spectra of a semiconductor QD-cavity system driven via on-resonance exciton pumping ($\omega_L = \omega_x$, with $\Delta_{cx} = 2$ meV) for various values of the exciton pump η_x and phonon-bath temperature T. The black line shows spectra obtained from a weak-coupling master equation, the blue line from a polaronic master equation, and the red line from the variational master equation developed in this work. In all plot, the frequency is taken with respect to the QD emission and $g = 26.7$ μeV is used.

frequency renormalization in the bottom right panel of Fig. 3 to those reported in Fig. 3(b) of Ref. [57] and Fig. 5 of Ref. [58]. There, a renormalization of ∼10% is reported for bare Rabi frequencies at the order of 1 meV, in agreement with our simulations from the variational model, while such a renormalization obtained within the polaron approach reaches ∼35%, elucidating overvaluation of the thermal effects. It is worth mentioning that in spite of discrepancies regarding its magnitude, all three models account for the phonon-assisted cavity feeding phenomenon.

VI. CONCLUSION

In this work we have derived an optimized master equation for a quantum photon emitter simultaneously coupled to a phonon bath and to an optical resonator, inspired by the polaronic transformation but with phonon displacements vari-

ationally determined by a mode-dependent approach. Thus, a theory flexible enough to encompass the weak-coupling and polaronic methods, but applicable on a larger range of experimental conditions, was obtained.

We applied the developed theory in the simulation of the resonance fluorescence emission from a single quantum dot embedded in a high-quality microcavity, for different temperature and excitation values. Such spectra were also calculated within the weak-coupling and conventional polaronic theories so that a pertinent comparison could be carried out among the three models considered. The numerical results showed that in comparison to the more rigorous variational approach, the weak-coupling and polaronic theories correspondingly overestimate the phonon dissipative effects as the temperature and the excitation power increase.

In conclusion, the variational master equation obtained here is expected to provide a valuable tool to simulate and

explain experiments on solid-state emitters interacting with phonon reservoirs and QED cavities, carried out under light-matter coupling, pumping rate, and temperature values lying in a much wider range than those spanned by previously available master equation approaches. This is of significance given the increasing excitation intensities and emitter-cavity mode couplings achieved in state-of-the-art quantum optical experiments.

[1] K. Murch, Cavity quantum electrodynamics: Beyond strong, Nat. Phys. **13**, 11 (2017).

[2] F. Yoshihara, T. Fuse, S. Ashhab, K. Kakuyanagi, S. Saito, and K. Semba, Superconducting qubit-oscillator circuit beyond the ultrastrong-coupling regime, Nat. Phys. **13**, 44 (2017).

[3] P. Forn-Díaz, J. J. García-Ripoll, B. Peropadre, J. L. Orgiazzi, M. A. Yurtalan, R. Belyansky, and A. Lupascu, Ultrastrong coupling of a single artificial atom to an electromagnetic continuum in the nonperturbative regime, Nat. Phys. **13**, 39 (2017).

[4] I. Chiorescu, P. Bertet, K. Semba, Y. Nakamura, C. J. P. M. Harmans, and J. E. Mooij, Coherent dynamics of a flux qubit coupled to a harmonic oscillator, Nature (London) **431**, 159 (2004).

[5] J. Heo, M. S. Kang, C. H. Hong, S. G. Choi, and J. P. Hong, Scheme for swapping two unknown states of a photonic qubit and an electron-spin qubit using simultaneous quantum transmission and teleportation via quantum dots inside single-sided optical cavities, Phys. Lett. A **381**, 1845 (2017).

[6] R. J. Coles, D. M. Price, B. Royall, E. Clarke, M. S. Skolnick, A. M. Fox, and M. N. Makhonin, Path-dependent initialization of a single quantum dot exciton spin in a nanophotonic waveguide, Phys. Rev. B **95**, 121401(R) (2017).

[7] A. Stockklauser, P. Scarlino, J. V. Koski, S. Gasparinetti, C. K. Andersen, C. Reichl, W. Wegscheider, T. Ihn, K. Ensslin, and A. Wallraff, Strong Coupling Cavity QED with Gate-Defined Double Quantum Dots Enabled by a High Impedance Resonator, Phys. Rev. X **7**, 011030 (2017).

[8] S. Dufferwiel, T. P. Lyons, D. D. Solnyshkov, A. A. P. Trichet, F. Withers, S. Schwarz, G. Malpuech, J. M. Smith, K. S. Novoselov, M. S. Skolnick, D. N. Krizhanovskii, and A. I. Tartakovskii, Valley-addressable polaritons in atomically thin semiconductors, Nat. Photon. **11**, 497 (2017).

[9] H. Z. Song, M. Hadi, Y. Zheng, B. Shen, L. Zhang, Z. Ren, R. Gao, and Z. M. Wang, InGaAsP/InP nanocavity for single-photon source at 1.55-μm telecommunication band, Nanoscale Res. Lett. **12**, 128 (2017).

[10] X. Ding, Y. He, Z. C. Duan, N. Gregersen, M. C. Chen, S. Unsleber, S. Maier, C. Schneider, M. Kamp, S. Höfling, C. Y. Lu, and J. W. Pan, On-Demand Single Photons with High Extraction Efficiency and Near-Unity Indistinguishability from a Resonantly Driven Quantum Dot in a Micropillar, Phys. Rev. Lett. **116**, 020401 (2016).

[11] S. Unsleber, Y. M. He, S. Gerhardt, S. Maier, C. Y. Lu, J. W. Pan, N. Gregersen, M. Kamp, C. Schneider, and S. Höfling, Highly indistinguishable on-demand resonance fluorescence photons from a deterministic quantum dot micropillar device with 74% extraction efficiency, Opt. Express **24**, 8539 (2016).

[12] H. Wang, Z. C. Duan, Y. H. Li, S. Chen, J. P. Li, Y. M. He, M. C. Chen, Y. He, X. Ding, C. Z. Peng, C. Schneider, M. Kamp, S. Höfling, C. Y. Lu, and J. W. Pan, Near-Transform-Limited Single Photons from an Efficient Solid-State Quantum Emitter, Phys. Rev. Lett. **116**, 213601 (2016).

[13] S. M. Ulrich, S. Ates, S. Reitzenstein, A. Löffler, A. Forchel, and P. Michler, Dephasing of Triplet-Sideband Optical Emission of a Resonantly Driven InAs/GaAs Quantum Dot Inside a Microcavity, Phys. Rev. Lett. **106**, 247402 (2011).

[14] F. Hargart, K. Roy-Choudhury, T. John, S. L. Portalupi, C. Schneider, S. Höfling, M. Kamp, S. Hughes, and P. Michler, Probing different regimes of strong field light-matter interaction with semiconductor quantum dots and few cavity photons, New J. Phys. **18**, 123031 (2016).

[15] S. Ates, S. M. Ulrich, S. Reitzenstein, A. Löffler, A. Forchel, and P. Michler, Post-Selected Indistinguishable Photons from the Resonance Fluorescence of a Single Quantum Dot in a Microcavity, Phys. Rev. Lett. **103**, 167402 (2009).

[16] M. Calic, P. Gallo, M. Felici, K. A. Atlasov, B. Dwir, A. Rudra, G. Biasiol, L. Sorba, G. Tarel, V. Savona, and E. Kapon, Phonon-Mediated Coupling of InGaAs/GaAs Quantum-Dot Excitons to Photonic Crystal Cavities, Phys. Rev. Lett. **106**, 227402 (2011).

[17] A. Majumdar, E. D. Kim, Y. Gong, M. Bajcsy, and J. Vučković, Phonon mediated off-resonant quantum dot-cavity coupling under resonant excitation of the quantum dot, Phys. Rev. B **84**, 085309 (2011).

[18] D. P. McCutcheon, N. S. Dattani, E. M. Gauger, B. W. Lovett, and A. Nazir, A general approach to quantum dynamics using a variational master equation: Application to phonon-damped Rabi rotations in quantum dots, Phys. Rev. B **84**, 081305 (2011).

[19] K. Müller, K. A. Fischer, A. Rundquist, C. Dory, K. G. Lagoudakis, T. Sarmiento, Y. A. Kelaita, V. Borish, and J. Vučković, Ultrafast Polariton-Phonon Dynamics of Strongly Coupled Quantum Dot-Nanocavity Systems, Phys. Rev. X **5**, 031006 (2015).

[20] K. A. Fischer, K. Müller, A. Rundquist, T. Sarmiento, A. Y. Piggott, Y. Kelaita, C. Dory, K. G. Lagoudakis, and J. Vučković, Self-homodyne measurement of a dynamic Mollow triplet in the solid state, Nat. Photon. **10**, 163 (2017).

[21] S. Seyfferle, F. Hargart, M. Jetter, E. Hu, and P. Michler, Signatures of single-photon interaction between two quantum dots located in different cavities of a weakly coupled double microdisk structure, Phys. Rev. B **97**, 035302 (2018).

[22] H. Wang, W. Li, X. Jiang, Y. M. He, Y. H. Li, X. Ding, M. C. Chen, J. Qin, C. Z. Peng, C. Schneider, M. Kamp, W. J. Zhang, H. Li, L. X. You, Z. Wang, J. P. Dowling, S. Höfling, C. Y. Lu, and J. W. Pan, Toward Scalable Boson Sampling with Photon Loss, Phys. Rev. Lett. **120**, 230502 (2018).

[23] L. Hanschke, K. A. Fischer, S. Appel, D. Lukin, J. Wierzbowski, S. Sun, R. Trivedi, J. Vučković, J. J. Finley, and K. Müller, Quantum dot single-photon sources with ultra-low multi-photon probability, npj Quantum Inf. **4**, 43 (2018).

[24] Y. Y. Liu, K. D. Petersson, J. Stehlik, J. M. Taylor, and J. R. Petta, Photon Emission from a Cavity-Coupled Double Quantum Dot, Phys. Rev. Lett. **113**, 036801 (2014).

[25] Y. Y. Liu, J. Stehlik, C. Eichler, M. J. Gullans, J. M. Taylor, and J. R. Petta, Semiconductor double quantum dot micromaser, Science **347**, 285 (2015).

[26] J. S. Rojas-Arias, B. A. Rodríguez, and H. Vinck-Posada, Magnetic control of dipolaritons in quantum dots, J. Phys.: Condens. Matter **28**, 505302 (2016).

[27] J. Cotrino-Lemus and H. Y. Ramírez, Efficiently tunable photon emission from an optically driven artificial molecule, J. Phys.: Conf. Ser. **864**, 012081 (2017).

[28] M. S. Domínguez, D. F. Macias-Pinilla, and H. Y. Ramírez, Dipolariton formation in quantum dot molecules strongly coupled to optical resonators, J. Nanomater. 2018, 7916823 (2018), arXiv:1609.05525v3.

[29] E. Sim, Quantum dynamics for a system coupled to slow baths: On-the-fly filtered propagator method, J. Chem. Phys. **115**, 4450 (2001).

[30] A. Vagov, M. D. Croitoru, V. M. Axt, T. Kuhn, and F. M. Peeters, Nonmonotonic Field Dependence of Damping and Reappearance of Rabi Oscillations in Quantum Dots, Phys. Rev. Lett. **98**, 227403 (2007).

[31] A. Vagov, M. D. Croitoru, M. Glässl, V. M. Axt, and T. Kuhn, Real-time path integrals for quantum dots: Quantum dissipative dynamics with superohmic environment coupling, Phys. Rev. B **83**, 094303 (2011).

[32] D. G. Nahri, F. H. Mathkoor, and C. H. Raymond Ooi, Real-time path-integral approach for dissipative quantum dot-cavity quantum electrodynamics: Impure dephasing-induced effects, J. Phys.: Condens. Matter **29**, 055701 (2017).

[33] S. Kreinberg, W. W. Chow, J. Wolters, C. Schneider, C. Gies, F. Jahnke, S. Höfling, M. Kamp, and S. Reitzenstein, Emission from quantum-dot high-β microcavities: Transition from spontaneous emission to lasing and the effects of superradiant emitter coupling running title: Quantum-dot high-β microcavities, Light Sci. Appl. **6**, e17030 (2017).

[34] D. Suter, *The Physics of Laser-Atom Interactions* (Cambridge University Press, Cambridge, 1997), Vol. 19.

[35] C. Roy and S. Hughes, Polaron master equation theory of the quantum-dot Mollow triplet in a semiconductor cavity-QED system, Phys. Rev. B **85**, 115309 (2012).

[36] R. Silbey and R. A. Harris, Variational calculation of the dynamics of a two level system interacting with a bath, J. Chem. Phys. **80**, 2615 (1984).

[37] A. L. Kuzemsky, Variational principle of Bogoliubov and generalized mean fields in many-particle interacting systems, Int. J. Mod. Phys. B **29**, 1530010 (2015).

[38] A. Nazir and D. P. McCutcheon, Modelling exciton-phonon interactions in optically driven quantum dots, J. Phys.: Condens. Matter. **28**, 103002 (2016).

[39] M. A. Schlosshauer, *Decoherence: And the Quantum-to-Classical Transition* (Springer, Berlin, 2007).

[40] C. Roy and S. Hughes, Influence of Electron-Acoustic-Phonon Scattering on Intensity Power Broadening in a Coherently Driven Quantum-Dot-Cavity System, Phys. Rev. X **1**, 021009 (2011).

[41] C. Roy and S. Hughes, Phonon-Dressed Mollow Triplet in the Regime of Cavity Quantum Electrodynamics: Excitation-Induced Dephasing and Nonperturbative Cavity Feeding Effects, Phys. Rev. Lett. **106**, 247403 (2011).

[42] H. Carmichael, *An Open Systems Approach to Quantum Optics*, Lecture Notes in Physics Monographs (Springer, Berlin, 2009), Vol. 18.

[43] R. J. Glauber, Coherent and incoherent states of the radiation field, Phys. Rev. **131**, 2766 (1963).

[44] Z. Harsij, M. B. Harouni, R. Roknizadeh, and M. H. Naderi, Influence of electron-phonon interaction on the optical spectrum and quantum statistics in a quantum-dot-cavity system: Master-equation approach, Phys. Rev. A **86**, 063803 (2012).

[45] M. B. Harouni, R. Roknizadeh, and M. H. Naderi, Influence of phonons on exciton-photon interaction and photon statistics of a quantum dot, Phys. Rev. B **79**, 165304 (2009).

[46] H. Y. Ramírez, Double dressing and manipulation of the photonic density of states in nanostructured qubits, RSC Adv. **3**, 24991 (2013).

[47] Y. He, Y. M. He, J. Liu, Y. J. Wei, H. Y. Ramírez, M. Atatüre, C. Schneider, M. Kamp, S. Höfling, C. Y. Lu, and J. W. Pan, Dynamically Controlled Resonance Fluorescence Spectra from a Doubly Dressed Single InGaAs Quantum Dot, Phys. Rev. Lett. **114**, 097402 (2015).

[48] B. Krummheuer, V. M. Axt, and T. Kuhn, Theory of pure dephasing and the resulting absorption line shape in semiconductor quantum dots, Phys. Rev. B **65**, 195313 (2002).

[49] E. M. Gauger, A. Nazir, S. C. Benjamin, T. M. Stace, and B. W. Lovett, Robust adiabatic approach to optical spin entangling in coupled quantum dots, New J. Phys. **10**, 073016 (2008).

[50] H. J. Carmichael and M. O. Scully, Statistical Methods in Quantum Optics 1: Master Equations and Fokker-Planck Equations, Phys. Today **53** (3), 78 (2000).

[51] S. M. Tan, A computational toolbox for quantum and atomic optics, J. Opt. B **1**, 424 (1999).

[52] J. I. Perea, D. Porras, and C. Tejedor, Dynamics of the excitations of a quantum dot in a microcavity, Phys. Rev. B **70**, 115304 (2004).

[53] H. C. Kim, T. C. Shen, K. Roy-Choudhury, G. S. Solomon, and E. Waks, Resonant Interactions between a Mollow Triplet Sideband and a Strongly Coupled Cavity, Phys. Rev. Lett. **113**, 027403 (2014).

[54] A. J. Ramsay, A. V. Gopal, E. M. Gauger, A. Nazir, B. W. Lovett, A. M. Fox, and M. S. Skolnick, Damping of Exciton Rabi Rotations by Acoustic Phonons in Optically Excited InGaAs/GaAs Quantum Dots, Phys. Rev. Lett. **104**, 017402 (2010).

[55] A. J. Ramsay, T. M. Godden, S. J. Boyle, E. M. Gauger, A. Nazir, B. W. Lovett, and M. S. Skolnick, Phonon-Induced Rabi-Frequency Renormalization of Optically Driven Single InGaAs/GaAs Quantum Dots, Phys. Rev. Lett. **105**, 177402 (2010).

[56] Y. J. Wei, Y. He, Y. M. He, C. Y. Lu, Y. W. Pan, C. Schneider, M. Kamp, S. Höfling, D. P. McCutcheon, and A. Nazir, Temperature-Dependent Mollow Triplet Spectra from

a Single Quantum Dot: Rabi Frequency Renormalization and Sideband Linewidth Insensitivity, Phys. Rev. Lett. **113**, 097401 (2014).

[57] M. Glässl, L. Sörgel, A. Vagov, M. D. Croitoru, T. Kuhn, and V. M. Axt, Interaction of a quantum-dot cavity system with acoustic phonons: Stronger light-matter coupling can reduce the

visibility of strong coupling effects, Phys. Rev. B **86**, 035319 (2012).

[58] A. Vagov, M. Glässl, M. D. Croitoru, V. M. Axt, and T. Kuhn, Competition between pure dephasing and photon losses in the dynamics of a dot-cavity system, Phys. Rev. B **90**, 075309 (2014).